

Fast Optical Form Measurements of Rough Cylindrical and Conical Surfaces in Diesel Fuel Injection Components

Thomas J. Dunn, Robert Michaels, Simon Lee, Mark Tronolone, and Andrew Kulawiec;
Corning Tropol Corporation, Fairport, NY

1.0 Introduction

The requirements for a more efficient diesel engine with lower emissions have driven the form tolerances for fuel injectors beyond the limits of the automotive industry's current metrology capabilities. In order to generate the required pressure levels for fuel injection, the manufacturing tolerances for the cylindrical and conical surfaces of fuel injector components need to be monitored with sub micron resolution and accuracy. This is particularly difficult when the surfaces to be measured are buried deep within a blind hole where access is limited. An optical metrology system is preferred to allow rapid measurement suitable for a production environment; however, the surface roughness of the components exceeds the optical wavelengths used in most conventional instruments.

We present a new instrument in which form and geometry measurements of rough cylindrical and conical surfaces are made using a dual-wavelength interferometer system. The system uses two solid-state lasers at different wavelengths to extend the dynamic range of measurement to accommodate the surface roughness of the cylindrical and conical forms to be measured. The two laser beams are combined and sent through a unique probe that can deliver the beams to the desired measurement surface at the bottom of a 3.5 mm diameter by 45 mm deep blind hole. In this paper, we provide a description of the system's design, and present some measurement results that manifest its unique capabilities.

2.0 System Design

The heart of the new instrument is the dual wavelength interferometer system. One interferometer operates at 1310 nm and the second operates at 1550 nm. When the interferometric patterns at the two different fundamental wavelengths are analyzed together, a combined pattern with a synthetic wavelength of 8.46 μm is generated. Both interferometers are independently capable of measuring smooth parts and when the two wavelengths are used in conjunction, it is possible to measure ground parts with an R_z of 2 μm . Each interferometer uses a distributed feedback (DFB) solid-state laser as its source. The laser beam is split into a reference and measurement arm. The measurement arm is directed to the probe and focused onto the part to be measured. Light reflected from the part surface is imaged back through the probe and recombined with the reference arm in the sensor head (Fig. 2). The combined arms are imaged onto four



Figure 1. The new machine can measure rough cylindrical and conical surfaces inside of blind holes.

different detectors with an induced incremental 90-degree phase shift among them. A surface height map is generated from instantaneous phase measurements taken at individual points on the part as the focused beam is scanned over the part surface.

The machine employs a unique probe design that allows the test arms of both interferometers to be delivered to the bottom of a 3.5 mm diameter by 45 mm deep blind hole (Fig. 3). The probe includes miniature optics that split the test arms into two different beams. Each beam leaves the probe at a different angle for measuring two different surfaces: it may be a cone, a cylinder, or a flat. Both beams contain both wavelengths, but only one beam can be used for measurements at a time. Since each probe is capable of measuring at two different angles, relational measurements can be performed among different regions of the part such as runout, co-axiality, or perpendicularity. There are two different types of probes that have already been used with this machine: a cylinder-cone probe that is capable of measuring cylinders and cones with a 60 degree cone angle; and a cylinder-flat probe capable of measuring cylinders and flats. We are currently working on development for smaller diameter probes as well as for probes with different cone angles.

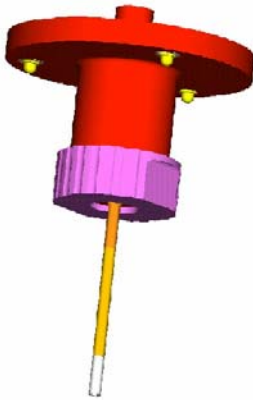


Figure 3. The probe has miniaturized optics at the bottom of the probe stem.

The bracket also incorporates a mechanical shutter to block the laser beam and detection electronics to prevent stage motion in case of improper probe loading.

The depth of focus of the optical probe is about 40 μm . Motion profiles are optimized for each region on the part and for each type of part. The stages are mechanical crossed roller bearing stages with 2 mm pitch roller screws. The Z-stage has 180 mm of travel while the X-stage has 80 mm of travel. The stages are driven by brushless, slotless DC motors with integral encoders. The stages move the probe along the desired motion profile determined by the software in the computer. Since the stage motion is neither perfectly smooth nor straight, a three-axis displacement measuring interferometer is used to monitor the stage motion. There are two Zerodur “stick” mirrors mounted to the X-Z stage. A frequency-stabilized helium-neon laser beam is reflected from the Zerodur mirrors to



Figure 2. The sensor head contains the DFB laser, optics, detectors, and electronics.

Figure 4 shows the sensors and the two-angle probe mounted onto a rigid baseplate that rides on an X-Z stage system. Mirrors are used to combine the beams from the two sensors and direct them into the probe. The probe is mounted in a kinematic bracket with a magnetic preload that allows the probe to be removed and re-inserted so that it still maintains alignment.

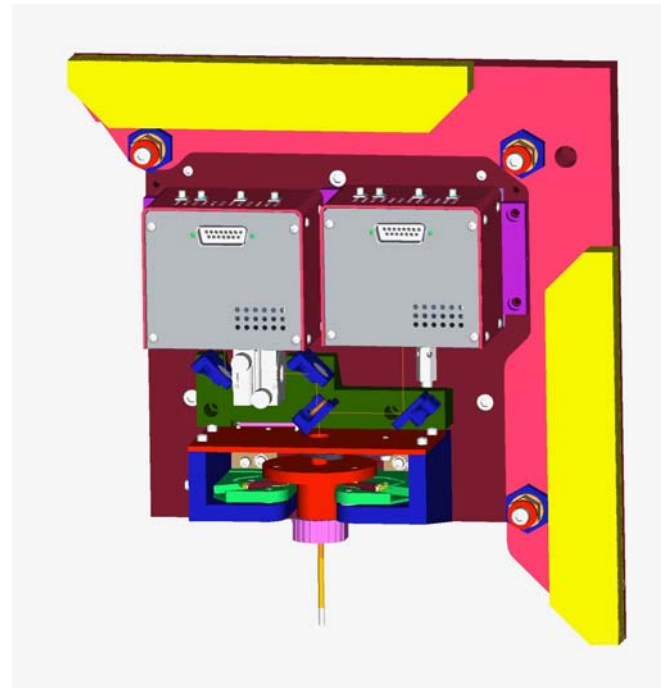


Figure 4. The sensors, probe, and stick mirrors are mounted on a rigid base plate which is carried by the X-Z stage system to move the focused laser beam along the surface of the part.

measure the straightness, yaw, and displacement errors of the stage motion. This data is recorded along with the phase data to remove errors caused by the stage motion.

The components to be measured are manually mounted to the air-bearing spindle by a hydraulic expansion chuck. The action of the chuck is very repeatable eliminating active alignment of the part to the spindle. The residual tilt and decenter of the part (typically less than several microns) is removed after the measurement during the software analysis. The air-bearing spindle rotates at 600 RPM and is powered by a direct-drive, brushless, DC motor with an integral high-resolution encoder. The quadrature signals from the spindle encoder are used to clock the data acquisition during the measurement. The data is simultaneously acquired from 8 channels from the two IR sensors and 3 channels from the HeNe displacement measuring interferometer.

For maximum measurement accuracy and repeatability, the entire measurement system is mounted on a granite base and riser block as shown in Fig. 5. The X-Z stage assembly is mounted on the riser block and the spindle is mounted in a hole through the base section. The granite structure is integrated into a cradle supported by a pneumatic isolation frame for increased immunity from external vibrational sources.

The external enclosure shown in Fig. 1 has two separate sections. The computer and control electronics are mounted within a cabinet that is rigidly attached to the enclosure and yet isolated from the temperature controlled environment. The operator accesses the chuck through a pneumatically controlled door operated by a foot switch. Space is also provided so that numerous parts, probes, fixtures, and calibration artifacts can all be stored in drawers, which are maintained at the same temperature as the measurement area. The enclosure serves as an environmental chamber to keep the entire measurement area at a constant temperature to within ± 0.25 degrees Celsius. The environmental control system consists of a solid-state thermoelectric cooler and heater, a blower assembly, and control and monitoring electronics positioned at various locations throughout the enclosure.

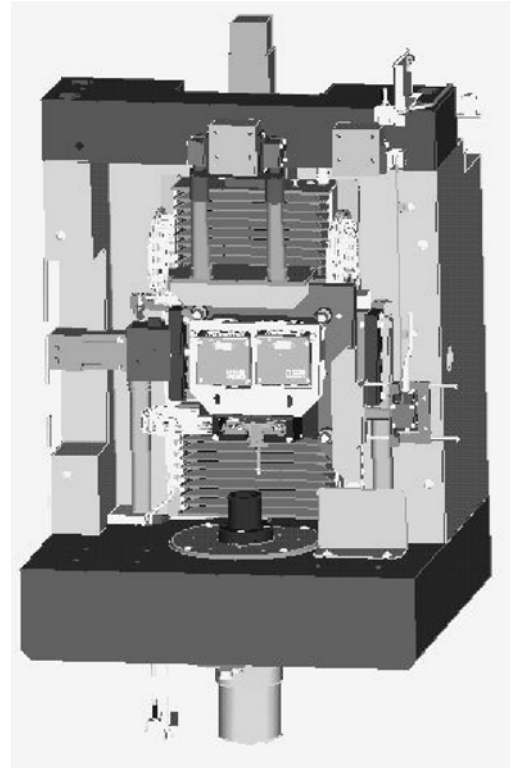


Figure 5. The stacked X-Z stage system is mounted to the vertical granite riser, and the spindle is mounted to the granite base.

3.0 Measurement Results

Figure 6 shows the two measurement regions of interest as well as the aspect ratio for the inside of the fuel injector nozzle. The conical section is about 1.5 mm high while the cylindrical section is 10 mm high. We show in Fig. 7 the measurement results from the inside cone of a fuel injector nozzle. This region lies at the bottom of the 40 mm blind hole and we are able to see the spray holes of the nozzle through which the fuel is injected. Fig. 7a shows the raw interferometric data including the tilt and decenter that results from the manual loading of the part into the collet. The part was spun at 600 RPM and the stage speed was chosen so that the spiral step size was 4 μm . This gives an array of 358 X 1024 points to cover this conic section. Fig. 7b shows the 3-D and 2-D plots of the same data set after the tilt and decenter was removed. Since the probe tip is scanned along a line parallel to the surface of the cone, an ideal part would be displayed in our software as a cylinder. The conical shape shown in Fig. 7b is a result of the angular error in the manufacturing of this part. The raw cone data was analyzed with a 50% Gaussian filter using 50 UPR in the radial direction and 0.08 mm in the axial direction. For the cylinder

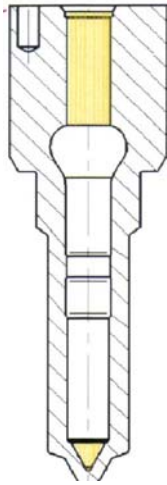


Figure 6. The measured regions of the fuel injector are highlighted.

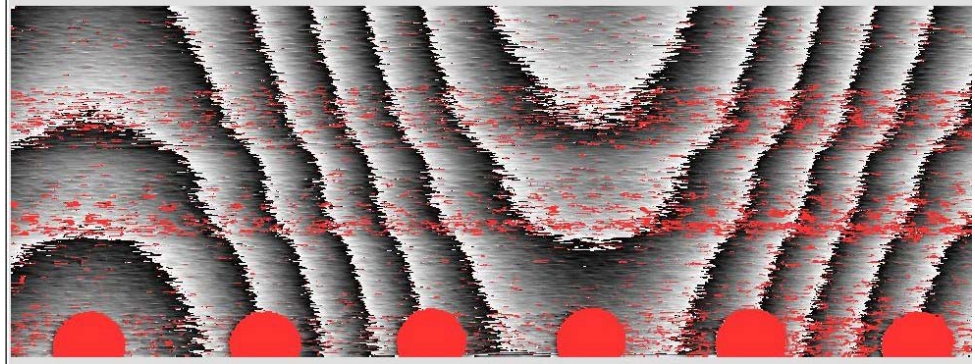


Figure 7a. The spray holes are seen in the interferometric data for the cone inside of the fuel injector

section the probe was scanned so that there was 50 μm between adjacent spiral scans resulting in a 225 X 1024 array after 0.2 mm edge exclusion. In this case the cylindrical data set was analyzed with a Gaussian filter using 50 UPR and 0.8 mm. Using the data from the cylindrical section of the part, we are able to establish a datum to determine the average radial runout over the entire cone. For this part the runout came to 2.6 μm .

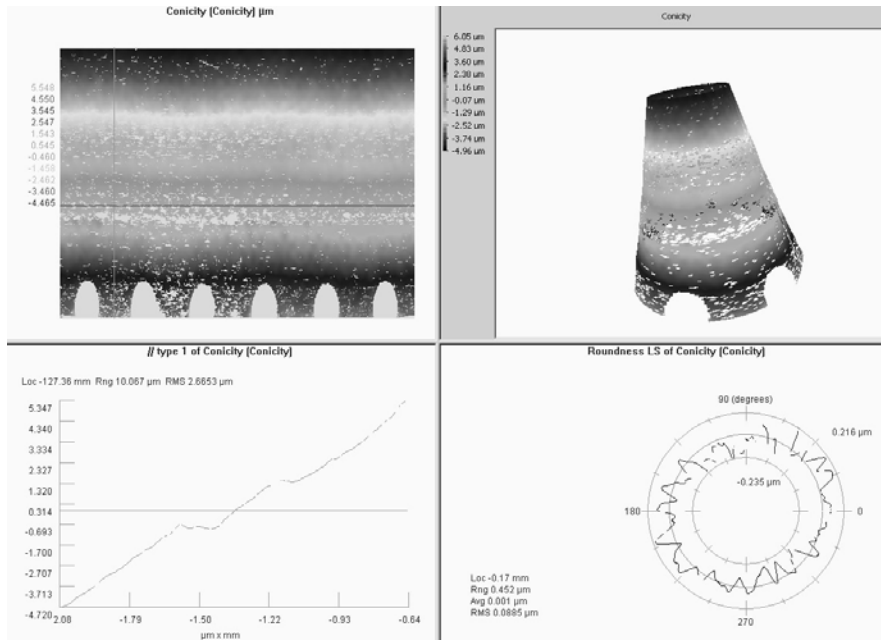


Figure 7b. Contour, 3-D, and 2-D plots are shown for the conical section inside of the fuel injector

The repeatability from this measurement technique is very high. We can typically achieve a standard deviation of 10 – 30 nm depending on the parameter being measured. We show in Fig. 8 the roundness results of the inside cone for 25 different parts measured 20 times over a period of 5 days. For this set of data the average standard deviation was 11 nm.

The accuracy of the measurements is verified through the use of artifacts certified at both NIST and PTB. We manufactured artifacts for each of the measured parameters:

roundness, straightness, parallelism, angle, diameter, and runout. We performed gauge studies comparing the measured values to the certified values and achieved an accuracy of 40 nm or better for each of these parameters. A gauge study would typically consist of 25 measurements of the artifact in which the artifact was removed and reloaded before each measurement. We show in Fig. 9 a 3-D plot of the measurement of the roundness artifact. The PTB certified value for this artifact was 2.87 μm as measured by a Talyrond 73, and we measured 2.90 μm with a standard deviation of 11 nm. Similar results were achieved with the other artifacts.

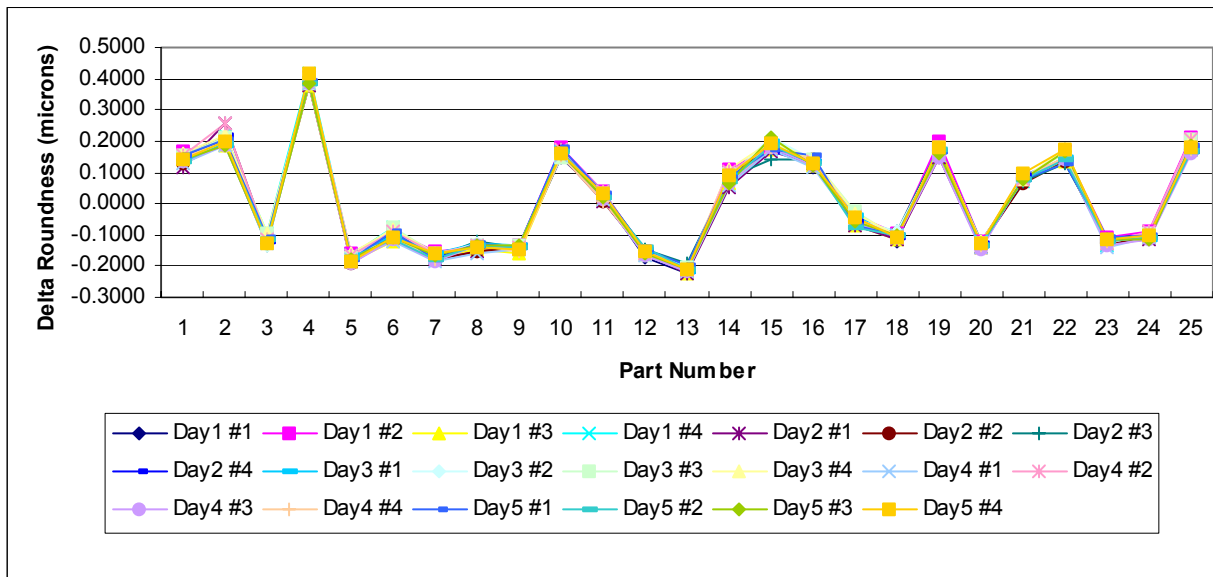


Figure 8. The roundness of 25 different fuel injector cones was measured 20 times over a period of 5 days. The average standard deviation over all of the measurements was 11 nm. Delta Roundness is the deviation of the measurement from the average roundness over all 25 parts.

Future efforts will be focused on the development of new types of probes that allow us to measure different cone angles and blind holes that have smaller diameters than the ones measured to date. In addition to automotive applications, we anticipate that this technology will address metrology needs for many other industries as well.

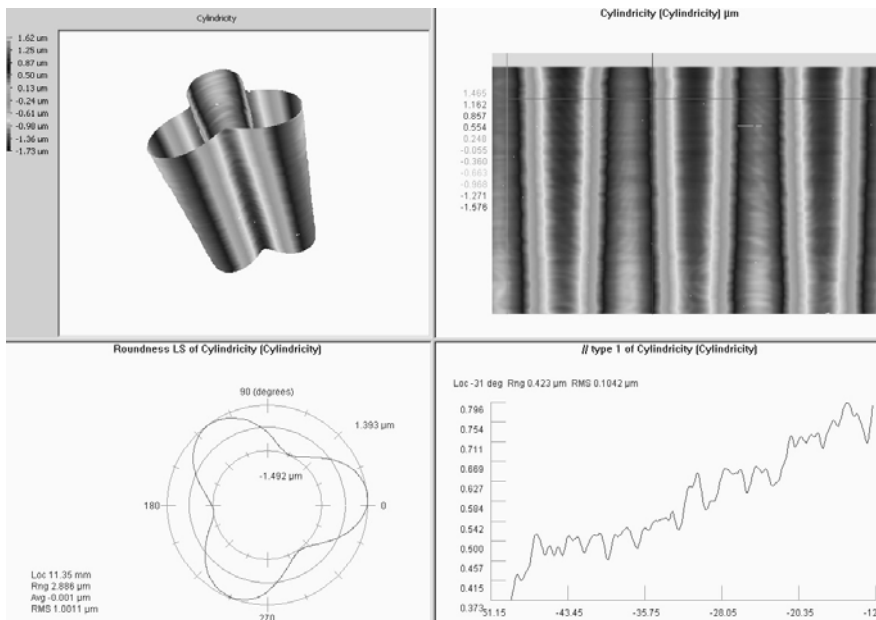


Figure 9. The roundness artifact was manufactured with three lobes. The difference between the certified and measured roundness is 30 nm.